Characteristics of Sulfuric Acid Condensation on Cylinder Liners of Large Two-Stroke Marine Engines

Cordtz, Rasmus Faurskov; Mayer, Stefan; Schramm, Jesper; Eskildsen, Svend S.

Publication date:
2014

Characteristics of Sulfuric Acid Condensation on Cylinder Liners of Large Two-Stroke Marine Engines

Rasmus Cordtz, Stefan Mayer, Jesper Schramm, Svend S. Eskildsen

Abstract

The present work seeks to clarify the characteristics of sulfuric acid condensation on the cylinder liner of a large two–stroke marine engine. The liner is directly exposed to the cylinder gas (i.e. no protective lube oil film) and is represented by a constant temperature over the full stroke. Formation of corrosive sulfuric acid in the cylinder gas is modeled with a calibrated engine model that incorporates a detailed sulfur reaction mechanism. Condensation of sulfuric acid follows the analogy between heat and mass transfer. Average bulk gas acid dew points are calculated by applying two-phase thermochemistry of the binary H_2O-H_2SO_4 system. Max dew points of typically more than 200 °C are modeled close to max pressure and variations in terms of operating conditions are not large. However small increments of the dew point provided by e.g. the residual gas fraction, operating pressure, sulfur content and charge air humidity acts to increase the surface area that is exposed to condensation. Depending on the actual liner temperature the deposition of sulfuric acid can be very sensitive to the operating strategy. A higher liner temperature theoretically provides the means to hamper sulfuric acid condensation.

1. Introduction

When Heavy Fuel Oil (HFO) including sulfur is burned in a marine engine the cylinder liner is exposed to gas products of sulfur trioxide (SO_3) and sulfur dioxide (SO_2) where the latter is the primary sulfur compound. According to thermodynamic considerations the bulk gas temperature is generally too high to form corrosive sulfuric acid (H_2SO_4). Yet H_2SO_4 may form at the cooled liner surface from an instant reaction between SO_3 and water vapor (H_2O) that is a major combustion product. Consequently SO_3 and H_2SO_4 are lumped together and the fraction of fuel sulfur that is converted to corrosive species is formulated by eq. 1. In practice the fraction accounts for a few percent but it varies with operating conditions and fuel sulfur content [1,2].

$$\varepsilon = \frac{[SO_3]}{[SO_3]+[SO_2]} \quad (1)$$

If the liner temperature is lower than the sulfuric acid dew point then a part of the H_2SO_4 and H_2O in the bulk gas condense according to the thermochemistry of the binary H_2O-H_2SO_4 system. Liner corrosion is especially coupled to H_2SO_4 condensation as deposited liquid acid accelerates the degradation of the cast iron liner materiel. In practice it is experienced that uncontrolled corrosion can severely reduce the life time of a cylinder liner. To hamper

corrosion commercial cylinder lube oils are blended with acid neutralizing base additives that combined with the lube oil dosing strategy provides the means to prevent corrosion.

The sulfuric acid dew point may be determined from empirical formulas [3,4] that correlate the temperature with the pressure of SO_3 and H_2O. However such correlations do not provide information about the share of condensing H_2SO_4 and H_2O. A more convenient approach for the present study is to apply the thermochemistry of the two-phase H_2O-H_2SO_4 system. Theoretical correlations of this type are based on thermodynamic properties of the components in the gas and liquid phase. Abel [5] was among the first to derive the vapor-phase above a liquid solution of sulfuric acid and water. He used the best available thermodynamic data at that time. The theoretical models have been improved over the years as the thermodynamic data have been gradually upgraded. Today several correlations are suggested [5-9]. In this work the quite recent work of Bosen & Engels [10] is used to describe the complex nature of the H_2O-H_2SO_4 system. The model treats ideal gasses above a liquid solution where the partial pressures p_i (index i refers to H_2O and H_2SO_4) are calculated from the general expression in eq. 2. χ_i is the liquid mole fraction, γ_i is an activity coefficient and p_i^0 is the vapor pressure of the pure substance [11,12]. The activity coefficient is derived from the NRTL (Non-Random Two Liquid model) equation [13] wherein adjustable parameters are fitted to reproduce experimental data of total pressure, vapor phase composition and liquid molar enthalpy. The experimental data are cited in the work of Bosen & Engels that describe the phase equilibrium of the H_2O-H_2SO_4 system up to 96 % m/m H_2SO_4 in the temperature range between 0 - 240 °C.

$$p_i(T, c_a) = x_i \gamma_i {p_i}^0 \quad (2)$$

According to Gibbs phase rule the two phase H_2O-H_2SO_4 system yields two degrees of freedom. For a liquid phase at a given acid strength (c_a) eq. 2 provides the saturation pressures of H_2SO_4 and H_2O at a defined temperature. If the procedure is reversed then known pressures of H_2SO4 and H_2O can be applied to the equation from which the dew point temperature and the condensing acid strength can be determined.

The present work does not address liner corrosion directly but seeks to clarify the characteristics of H_2SO_4 condensation. The cylinder liner is directly exposed to the cylinder gas. I.e. the influence of the protecting lube oil is not considered. Gas species concentrations are simulated with a calibrated engine model [1] that includes a detailed sulfur reaction mechanism [14]. The process of condensation is modeled as molecular gas diffusion through the gaseous boundary layer very close to the liner surface. For the purpose the analytic expressions of Müller [15] are used which are based on the analogy between heat and mass transfer. In his theoretical approach Müller implemented the theory of a semi permeable gas-liquid interface that acts to hamper condensation due to convective motions from the non-condensable gases. Moreover the expressions are derived from the assumption of fully developed turbulence that reasonably fits the conditions in a large two-stroke marine engine.

2. Engine Model

In cylinder species formation is simulated with a multizone engine model that is previously developed by the authors [1]. The model incorporates a detailed sulfur reaction mechanism [14] besides the extended Zeldovich mechanism [16] in order to simulate products of sulfur compounds, mayor C-H-O species and nitrogen oxides (NO). The fuel is composed by n-dodecane ($C_{12}H_{26}$) and non-bonded elemental sulfur.
In the multizone approach the complex nature of the diesel spray and flame is not directly modeled. Instead the model seeks to reproduce flame conditions by separating the overall

fuel mass in multiple burned gas zones with no spatial location (0D model). At each crank angle from the point of fuel ignition and until the combustion is completed a new burned zone is created where the fuel burns stoichiometrically with fresh gas. The fresh gas is composed by charge air (normally dry air) including residual gasses that remain in the cylinder after the scavenging process. The flame temperature of a burned zone is calculated from the assumption that the gas products are immediately equilibrated at the high temperature in the order of ≈2600-2700 K. Hereafter a burned zone is diluted with fresh gas every crank angle during the expansion stroke at a defined rate. No more fuel is added to a burned zone and no gas exchange is considered between burned zones either. Consequently the ratio of air to combustion products increases in the burned zones during expansion and meanwhile the mass of the fresh gas is reducing. In the published material [1] the fresh gas chemistry is assumed to be frozen. In the present work however the fresh gas is treated as a homogenous zone wherein chemical reactions are considered from the point where compression starts and until the exhaust valve opens. The subsequent scavenging process is not modeled. Instead the residual gas fraction is set as a model input.
Due to the absence of experimental SO_3 measurements the model is calibrated against exhaust gas concentrations of NO produced by the large two-stroke reference engine specified in Table 1. The engine represents a modern marine engine that operates according to a simulated propeller curve [17] and experimental operating data are used as model input.

Number of cylinders	4
Bore/stroke	500mm / 2200 mm
Max speed	123 RPM
Max power	7050 kW

Table 1. *Specifications of the reference (two-stroke) marine engine used to investigate the characteristics of sulfuric acid condensation on the cylinder liner.*

3. Engine Simulations

In service the large marine engines operate at different loads and with fuels of varying sulfur contents. Consequently a cylinder liner will be exposed to gas species of varying densities that alter the properties of sulfuric acid condensation. In order to limit the number of simulations a constant sulfur content of 2 % m/m is used in this work at the operating conditions representing 25 % and 100 % engine load. Moreover the residual gas fraction is set to 3 % and 6 % m/m as seen in Table 2 that holds the four studied base cases.

	load	rpm	Fuel S	x_{res}	p_{boost}	T_{air}	p_{max}	λ_t	ε^*
Case	%	rev/min	% m/m	% m/m	bar	°C	bar	-	%
1	100	123	2.0	6	3.8	37	167	2.13	2.70
2	100	123	2.0	3	3.8	37	172	2.32	2.74
3	25	78	2.0	6	1.5	33	89	2.47	3.65
4	25	78	2.0	3	1.5	33	90	2.67	3.69

*at exhaust valve opening

Table 2. *Studied cases used to investigate the characteristics of sulfuric acid condensation in a large marine engine.*

In a previous work [1] the rate of combustion was determined for the two engine loads in Table 2 by combining a measured cylinder pressure trace with the first law of thermodynamics. In this work the process is reversed and the “known” combustion rate is used to calcu-

late the cylinder pressure history. This is a fair approach due to the slight variations of the residual gas fraction. The cylinder pressure plays a key role as it significantly affects SO_3 formation [2] and alters the properties of condensation throughout the cycle. The modeled pressure histories are presented in Figure 1. When the residual gas fraction is increased the mass of trapped fresh gas reduces a little. This leads to a slight reduction of the pressure trace as seen for the two engine loads in Figure 1.

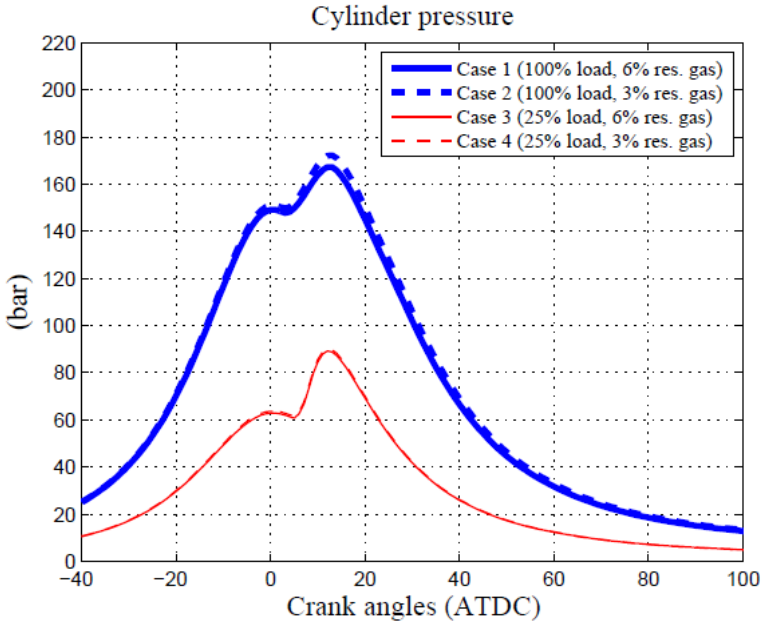

Figure 1. *Cylinder pressure traces of the studied cases in Table 2.*

4. Results

The ε-values defined in eq. 1 and listed in Table 2 describe the fraction of fuel sulfur that is converted to corrosive species at the point where the exhaust valve opens (EVO). Compared to the published material [1] the listed ε-values are slightly lower. This is explained by the implementation of improved experimental input data for the current engine simulations. Despite a higher operating pressure the ε-values are lowest at 100 % load. This reason for this is the lower engine speed at 25 % load that leaves more time for cylinder gas mixing which elevates the SO_3 formation [1, 2].

Modeled SO_3 concentrations over the expansion stroke are presented in Figure 2. Residual gasses from the prior engine cycle provide the initial SO_3 concentrations of less than 2 ppmv around TDC (Crank angles ATDC = 0). When the fuel sulfur burns SO_2 is the primary sulfur compound in the gas products. SO_3 forms at the expense of SO_2 during the expansion stroke at lower gas temperatures. However the governing SO_3 reactions are essentially quenched when the radical pool vanishes and final SO_3 concentrations are less than 20 ppmv.

Formation of H_2O reflects the fuel burn rate and H_2O exists in much higher concentrations than SO_3. As H_2O and SO_3 are formed under different thermal conditions the shape of their pressure traces are quite different as seen in Figure 2. Due to the operating conditions and the residual gas fraction the SO_3 pressure peaks in case 1 a little after TDC as seen in Figure 3. Otherwise the SO_3 pressure peaks some 50-80 CA ATDC when SO_3 is formed in the gas products.

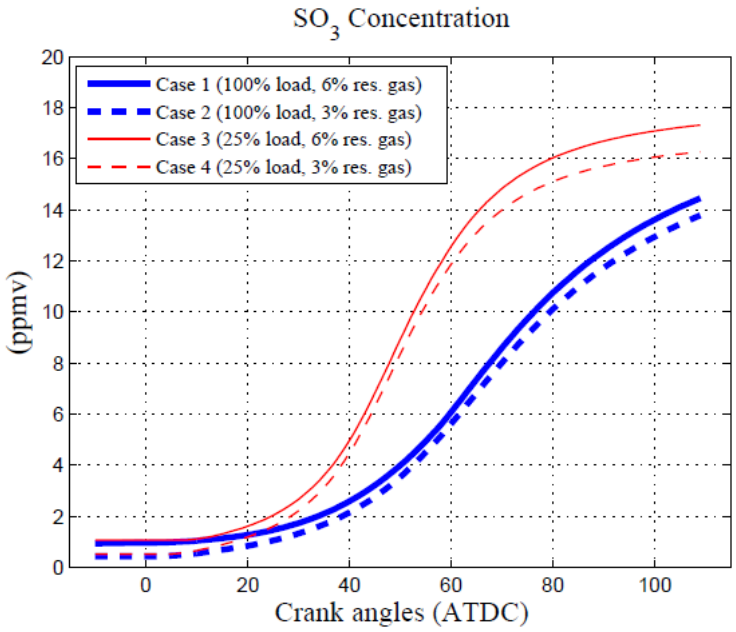

Figure 2. *Simulated SO_3 concentrations (average) of the studied cases in Table 2.*

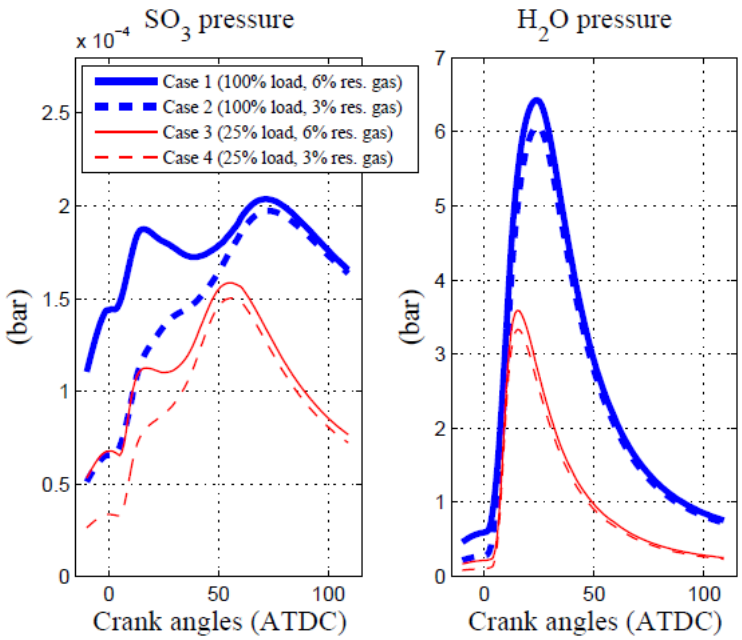

Figure 3. *Modeled SO_3 and H_2O pressures (average) of the studied cases in Table 2.*

The sulfuric acid dew points presented in Figure 4 are calculated with eq. 2 and are based on the SO_3 and H_2O pressure traces in Figure 3. Max dew points of typically more than 200 °C are located a little after TDC where the H_2O pressure is high. The ever reducing cylinder pressure during the expansion stroke provides that the acid dew point is comparably low even when SO_3 is formed in the cylinder gas (Fig. 2). Yet the acid dew point is strongly influ-

enced by the minor SO_3 concentrations as it clearly exceeds the dew point of H_2O as shown for case 1 and case 3 in Figure 4.
The dashed horizontal lines in Figure 4 represent constant liner temperatures of 170 °C and 210 °C that roughly correspond to 25 % and 100 % engine load respectively. The difference is rational but the liner temperature is highly variable in practice. It depends on the operating strategy and reduces from TDC and throughout the expansion stroke. Nevertheless the anticipated liner temperatures are reasonably applied to illustrate the characteristics of sulfuric acid condensation.
When the dew point is higher than the liner temperature sulfuric acid and water condense on the liner surface. Deposited liquid evaporates back into the gas phase if the dew point temperature is lower than the liner temperature. The liner area that is exposed to condensation scales with the number of crank angles between the point where condensation starts and stops. In case 3 the liner area is exposed to condensation from ≈5 - 70 CA ATDC. The higher liner temperature in case 1 provides that the exposed surface is comparably low (≈15 - 40 CA ATDC) despite a higher dew point trace. At both loads the exposed area increases slightly with the residual gas fraction and the exposed liner area can be reduced if the liner temperature is increased.
As shown in Figure 4 the dew point of H_2O remains lower than the anticipated liner temperatures. Consequently pure water does not condense on the liner under the given conditions. If pure water condenses the liquid acid will be highly diluted.

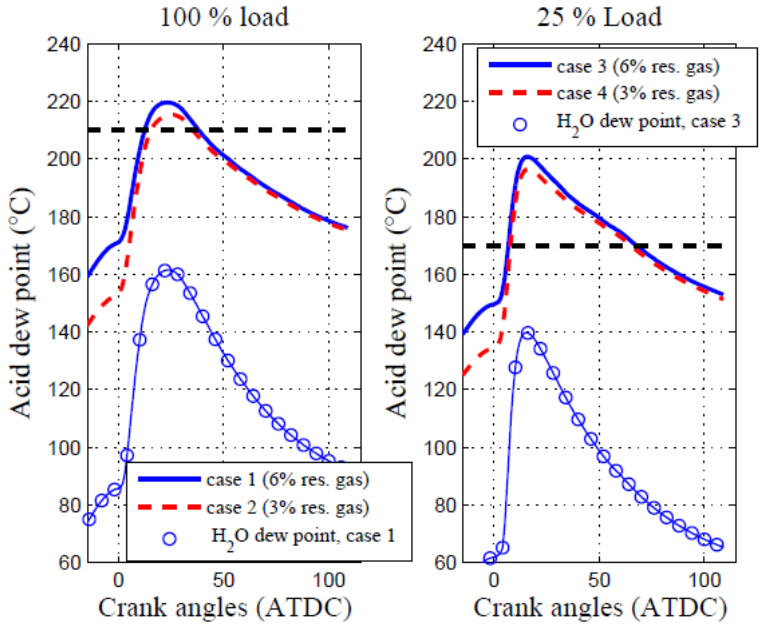

Figure 4. *Sulfuric acid dew points (average) of the studied cases in Table 2. The dashed horizontal lines represent constant cylinder liner temperatures of 170 °C and 210 °C.*

During a cycle the H_2O pressure is affected by the humidity of the intake air and the assumption of dry intake air conditions acts to underestimate real dew points since marine engines often operate in very humid environments. In Figure 5 the relative humidity (φ) of the intake air in case 3 is varied from 0 to 1. Engine simulations show that the SO_3 formation is weakly hampered by the humidity whereas the dew point temperature and the H_2O concentration is elevated as shown in Figure 5. The effect is most pronounced before TDC and the max dew point temperature is elevated ≈15 °C when the intake air is fully saturated instead of dry. In the remainder of the cycle the relative effect of the moist air reduces as H_2O forms

from the the fuel combustion. Nevertheless moist air increases the exposed liner area. At φ = 1 condensation of sulfuric acid initiates before TDC where the acid dew point exceeds the anticipated liner temp of 170 °C as seen in Figure 5.

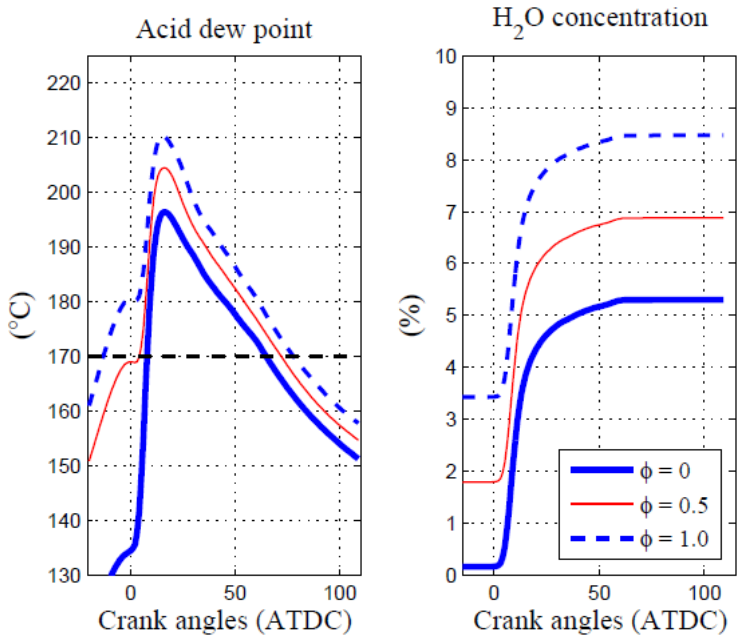

Figure 5. *Average sulfuric acid dew points and H_2O concentrations modeled at different intake air humidities (φ) for case 4 in Table 2. The dashed horizontal line represents a fixed cylinder liner temperature.*

The principles of condensation are illustrated in Figure 6. Close to the cooled liner surface SO_3 and H_2O from the bulk gas reacts instantly to form H_2SO_4. Together with H_2O the H_2SO_4 diffuses through the gaseous boundary layer to the gas liquid interface where the two compounds condense. Basically the H_2O and H_2SO_4 components are forced through the boundary layer due to partial pressure gradients. Transition from gas to liquid is not rate limiting [15] and phase equilibrium is assumed to exist at the interface.

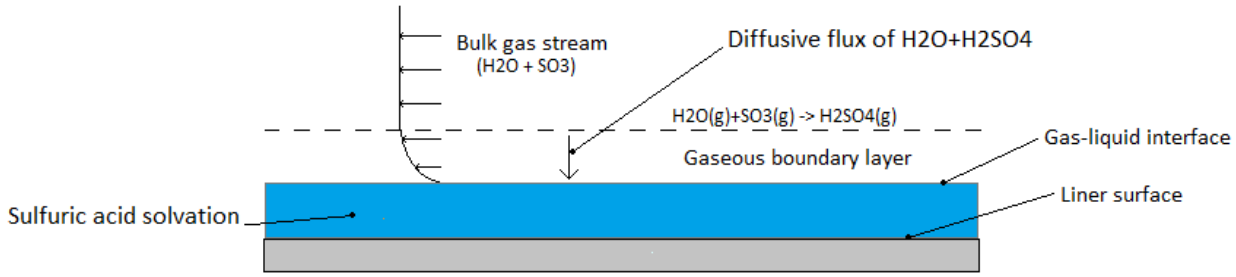

Figure 6. *The principles of H_2SO_4 and H_2O condensation on the cylinder liner.*

In order to determine the share of condensing H_2O and H_2SO_4 (eq. 2) one of these pressures are required at the gas liquid interface beside the liner temperature. The anticipated

liner temperatures are always higher than the dew point of H_2O and the H_2O contained in the bulk gas is orders of magnitude higher than the SO_3 content. As a result, the amount of H_2O that condenses together with H_2SO_4 is very small compared to the H_2O content in the bulk gas. For that reason the share of condensing H_2O and H_2SO_4 (acid strength) is reasonably determined (at each crank angle) from the assumption that the H_2O pressure at the gas-liquid interface equals the H_2O pressure in the bulk gas. Together with Müller's mass diffusion expressions in eq. 3 and 4 the condensing acid strength is used to calculate the condensation rates of H_2O and H_2SO_4. g_w and g_a denotes the transport/condensation rate of H_2O and H_2SO_4 respectively. In eq. 3 the H_2SO_4 pressure at the gas liquid interface ($p_{a,w}$) is found by applying the known acid strength (c_a) and the liner temperature to eq. 2. In eq. 4 the H_2O pressure at the interface ($p_{w,w}$) cannot be approximated by its pressure in the bulk gas ($p_{w,b}$) as before since one would have to evaluate ln(1)=0. Instead the definition of the condensing acid strength in eq. 5 is applied. Hereby the system of equations 3-5 that comprises the three unknowns g_a, g_w and $p_{w,w}$ can be solved.

Consistent with the heat and mass transfer analogy the rates in eq. 3 and 4 scale with the heat transfer coefficient (h) that is determined by Woschnis heat transfer correlation [16]. The coefficient is closely coupled to the system pressure and reduces throughout the expansion stroke after peaking around max pressure. The rate expressions also involve diffusion coefficients of H_2O and H_2SO_4 (k_w and k_a respectively). k_a is approximated by the binary diffusion coefficient of H_2SO_4 in a large excess of air [18] at 296 K (k_a = 0.08 atm cm^2 s^{-1}). Combined with the binary diffusion coefficient of H_2O in air [19] at 293 K (k_w = 0.260 atm cm^2 s^{-1}) the aspect ratio of k_w/k_a is around 3. If the coefficients are equally dependent on temperature and pressure the ratio is not altered throughout the engine cycle. In any case the condensation rates of the present study are highly independent of k_w/k_a ratios up to 100.

$$g_a = g_w \frac{k_w}{k_a}\frac{R_w}{R_a}\frac{\frac{p_{a,b}}{p}-\frac{p_{a,w}}{p}\left(\frac{p-p_{w,b}}{p-p_{w,w}}\right)^{\frac{k_w}{k_a}}}{1-\left(\frac{p-p_{w,b}}{p-p_{w,w}}\right)^{\frac{k_w}{k_a}}} \quad (3)$$

$$g_w = h\frac{R_g}{R_w c_{p,g}} ln\left(\frac{p-p_{w,w}}{p-p_{w,b}}\right) \quad (4)$$

$$c_a = \frac{g_a}{g_a+g_w} \quad (5)$$

Modeled rates of H_2SO_4 condensation over the expansion stroke are presented in Figure 7. A similar plot could be shown for H_2O condensation but is omitted. The condensation rates are expressed in mg/m^2 (deposited mass per exposed liner area) which means that the results of case 3 and 4 benefit from a lower engine speed compared to case 1 and 2. Condensation takes place when $g_a > 0$. When g_a is negative liquid H_2SO_4 evaporates from the liner surface and into the gas phase. In line with the dew point traces in Figure 4 the onset of

condensation is located a little after TDC in case 3 and 4. In case 1 and 2 the onset is "delayed" a few crank angles due to the higher liner temperature. With reference to the SO_3 concentrations in Figure 2 it is understood that the high condensation rates at ≈20 CA ATDC are realized by the SO_3 from the residual gasses combined with a high operating pressure and heat transfer rate. The rate reduces during the expansion stroke. However the deposition of acid increases significantly as the piston moves away from TDC due to the rapidly increasing surface area.
The liner temperature of 210 °C in case 1 and 2 provides that the evaporation of deposited sulfuric acid initiates before any significant SO_3 has yet been formed. A lower liner temperature involves more crank angles/time before the evaporation begins and the deposition of acid in case 3 and case 4 significantly profits from the SO_3 formed in the combustion products. As indicated in Figure 7 the rate of condensation represents large negative numbers during the gas compression (crank angles ATDC < 0) and late in the expansion stroke. Deposited acid will under the given conditions evaporate completely before condensation starts in the following cycle.

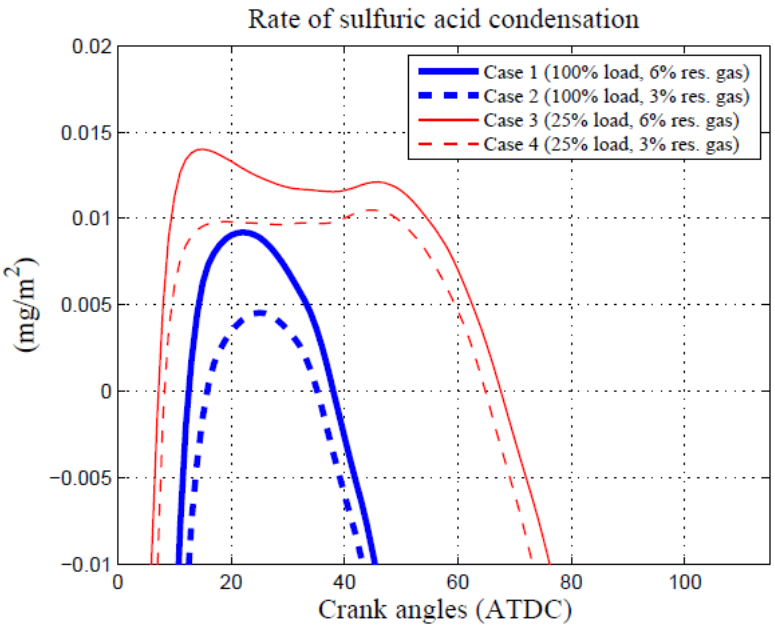

Figure 7. *Rate of H_2SO_4 condensation (average) on the cylinder liner for the studied cases in Table 2.*

To isolate the effect of the liner temperature in terms of sulfuric acid condensation the operating conditions of case 4 are used with two additional liner temperatures of 160 °C and 180 °C as seen in Figure 8. The initial deposition rates (around max pressure) are basically unchanged. However the traces in the figure illustrate that the exposed liner area is very sensitive to the liner temperature. At 160 °C condensation takes place over more than 80 crank angles ATDC. Moreover the impact from SO_3 formed in the current engine cycle increases when the liner temperature reduces. This is illustrated by the size of the peak rate that develops during the expansion stroke when temperature is lowered.

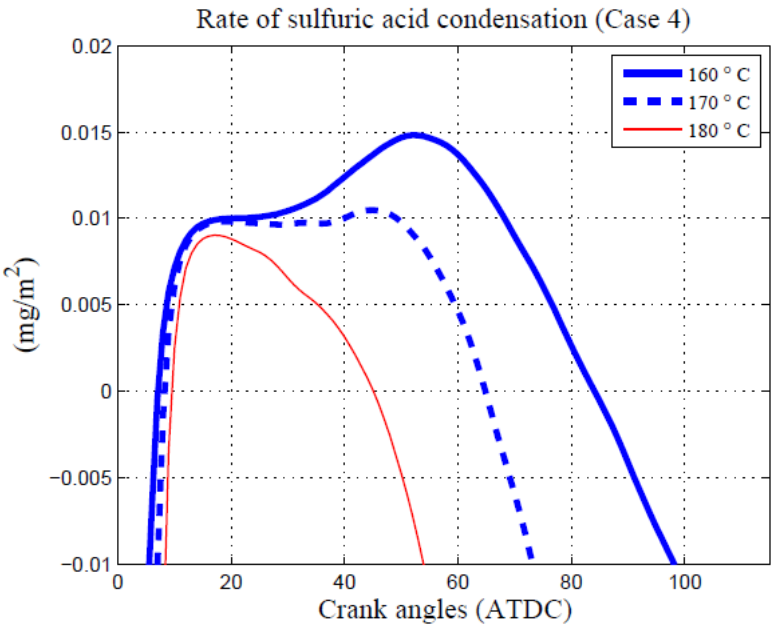

Figure 8. *Rate of H_2SO_4 condensation (average) on the cylinder liner for case 4 in Table 2. The legends refer to a constant liner temperature.*

The accumulated sulfuric acid mass over the expansion stroke until EVO are illustrated in Figure 9. The traces in the figure are at a max when the evaporation of acid begins. From the assumption that the condensate is uniformly distributed on the exposed liner area the following removal/evaporation of acid is completed after ≈20-25 crank angles as seen in the figure. The influence of the operating conditions becomes clearer when the peak points in Figure 9 are compared. At 100 % engine load (case 1 and 2) the high liner temperature provides that the exposed liner area is comparably small and the resulting acid mass is low. Nevertheless if the residual gas fraction is reduced from 6 % to 3 % the mass of condensate is reduced by ≈ 60 %. At 25 % engine load (case 3 and 4) the SO_3 forming in the combustion products significantly adds to the deposition of acid due to the lower liner temperature. At the same time the effect of the higher residual gas fraction is reduced to ≈22 %. The lower engine speed at 25 % engine load (Table 2) implies that the number of operating cycles is reduced by 1/3 relative to 100 % load. As a result the weight of case 3 and 4 should be reduced accordingly. Nonetheless the deposited mass per time unit will under the given conditions will still be several times higher at 25 % load.

Case 4^* in Figure 9 are based on the same operating conditions as case 4 but the liner temperature is reduced by 10 °C to 160 °C. The difference between case 4 and 4^* illustrates the influence of the temperature/exposed liner area. At the reduced temperature the deposited acid mass increases by a factor of more than 2 under the given conditions.

As shown in Figure 5 moisturized intake air elevates the exposed surface area through a higher dew point trace. Case 4^{**} in Figure 9 represents the same operating conditions as case 4 but the intake air is saturated. As illustrated the moist air basically doubles the deposited acid mass under the given conditions.

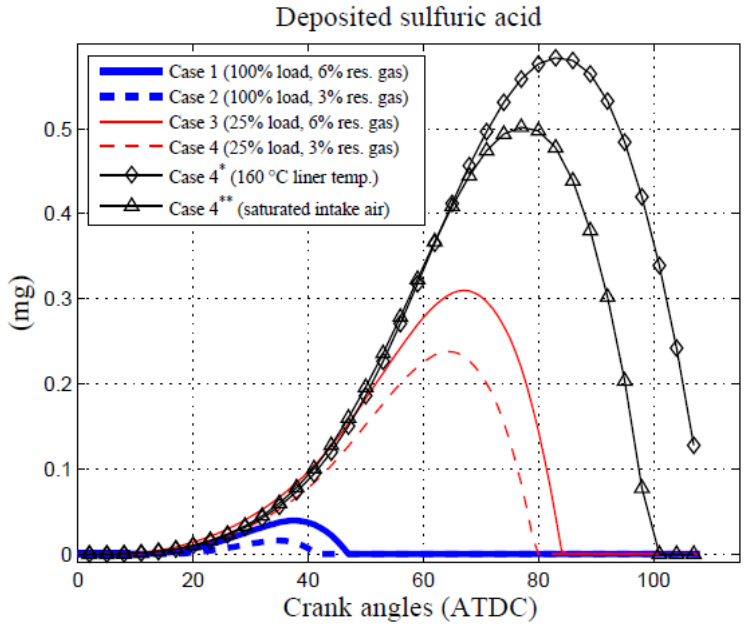

***Figure 9**. Deposited acid on the cylinder liner of the studied cases in Table 2. *The liner temperature is 160 °C instead of 170 °C. **The intake air is saturated.*

In Figure 10 the fraction of fuel sulfur that is converted to corrosive species (ε) at EVO is plotted against the fuel sulfur content. The results represent the operating conditions of case 4 in Table 2. In the typical fuel sulfur range from 1 - 4 % m/m the ε-value decreases slightly. As the sulfur content approaches very low numbers the ε-value tends to increase asymptotically, yet the presence of SO_3 in the cylinder gas will disappear in line with the vanishing sulfur content. Under the given conditions the combined effect of higher SO_3 pressures and exposed liner areas provides that the deposition of sulfuric acid scales with a quadratic regression of the sulfur content as illustrated in the figure.

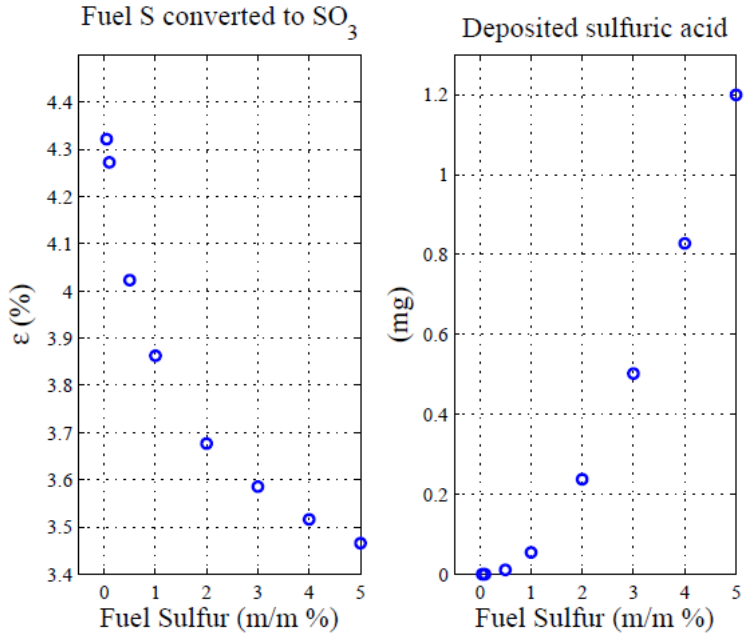

***Figure 10**. Fraction of fuel sulfur converted to corrosive species and deposited sulfuric acid on the cylinder during a cycle. The figures represent operating conditions at 25 % engine load.*

5. Discussion

With respect to sulfuric acid condensation on a marine engine cylinder liner the applied assumption of a homogenous cylinder gas mixture is not truly representative. The actual gas conditions of the mixing controlled combustion process are clearly heterogeneous in terms of composition and turbulence intensity etc. This challenges the modeled dew points and acid deposition rates. Moreover to the author's knowledge the applied thermochemistry of the H_2O-H_2SO_4 is system not directly validated against experimental measurements of sulfuric acid dew points.
In the present work the liner temperature is constant throughout the expansion stroke where condensation takes place. The actual temperature profile is highly variable. It depends on the operating strategy and reduces from TDC towards the bottom dead center. In practice the condensation of acid will strongly depend on the resulting liner temperature profile.
In this work the residual gas fraction and intake air humidity significantly alters the deposition of sulfuric acid. However if the actual liner temperature is generally lower than the acid dew point throughout the expansion stroke the influence of these conditions will decrease. In addition the accumulated acid mass on the liner can be considerably higher than predicted in this work because a larger liner area is exposed to condensation at lower liner temperatures.
A flue gas that contains SO_3 can form an acid mist if it is abruptly cooled below the acid dew point [20]. This may occur in practice when hot gas products reach the cooled liner surface. Mist formation is not treated in this work and the applied analogy between heat and mass transfer may overestimate the rate of acid condensation as the mist tends to stay in the bulk gas.

6. Conclusions

Formation of SO_3 in a large two-stroke marine engine is modeled with a multizone engine model and combined with diffusive mass transfer theory in order to examine the characteristics of sulfuric acid condensation on the cylinder liner. The liner is assumed to have a constant temperature over the full stroke. I.e. 170 °C and 210 °C at 25 % and 100 % engine load respectively. Sulfuric acid dew points are calculated from the thermochemistry of the two-phase H_2O-H_2SO_4 system. Acid dew points and condensation rates are based on a homogenous cylinder gas mixture. The reaction between H_2O and SO_3 instantly forms H_2SO_4 at the cooled liner surface. Thus SO_3 and H_2SO_4 are lumped together.
SO_3 from the residual gasses provides that the sulfuric acid dew point peaks close to max cylinder pressure at temperatures of typically more than 200 °C. Under the given conditions the condensation of sulfuric acid is very sensitive to the operating strategy. The operating pressure, fuel sulfur content and residual gas fraction elevates the SO_3 pressure that increases the rate of condensation as well as the acid dew point. When the dew point trace is elevated a larger liner area is exposed to condensation from which the deposition of acid can increase remarkably. Similarly the deposition increases with the charge air humidity.
In order to counteract condensation of acid the liner temperature is essential as it determines the size of the exposed liner area. Even a small reduction of the liner temperature will under the given conditions significantly increase the deposition of acid.

Nomenclature

Symbol		Unit
c_a	Condensing acid strength	kg/kg
$c_{p,g}$	Specific heat capacity of gas	J/kg-K
g_a	Rate of condensing sulfuric acid	mg/m^2-s
g_w	Rate of condensing water	mg/m^2-s
h	Heat transfer coefficient	W/m^2-K
k_a	Binary diffusion coefficient of H_2SO_4 in air	atm cm^2 /s
k_w	Binary diffusion coefficient of H_2O in air	atm cm^2 /s
$p_{a,b}$	Partial pressure of H_2SO_4 in bulk gas	Pa
$p_{a,w}$	Partial pressure of H_2SO_4 at gas-liquid interface	Pa
P_{boost}	Boost/charge air pressure	bar
$p_{w,b}$	Partial pressure of H_2O in bulk gas	Pa
$p_{w,w}$	Partial pressure of H_2O at gas-liquid interface	Pa
p_i^0	Vapor pressure of a pure substance	Pa
R_a	Specific gas constant of H_2SO_4	J/kg-K
R_w	Specific gas constant of H_2O	J/Kg-K
R_g	Specific gas constant of cylinder gas	J/Kg-K
T	Temperature	K
T_{air}	Charge air temperature	°C
x_i	Mole fraction in the liquid solvation	-
x_{res}	Residual gas fraction	% m/m
γ_i	Activity coefficient	-
ε	Fraction of fuel sulfur converted to SO_3	-
λ_t	Trapped excess air ratio	-

Abbreviations

ATDC	After top dead center
EVO	Exhaust valve opening
rpm	Revolutions per minute
S	Sulfur
TDC	Top dead center

Literature

[1] Cordtz, R.; Schramm, J.; Andreasen, A.; Eskildsen, S. S.; Mayer, S. Modeling the distribution of sulfur compounds in a large two stroke diesel engine. *Energy Fuels* **2013**, *27*, 1652-1660.

[2] Cordtz, R.; Schramm, J.; Rabe, R. Investigating SO_3 Formation from the Combustion of Heavy Fuel Oil in a Four-Stroke Medium-Speed Test Engine. *Energy and Fuels* **2013**, *27*.

[3] Verhoff, F. H.; Banchero, J. T. Predicting Dew Points of Flue Gases. *Chem. Eng. Prog.* **1974**, *70*, 71-72.

[4] Pierce, R. Estimating Acid Dewpoints in Stack Gases. *Chem. Eng.* **1977**, *84*, 125-128.

[5] Abel, E. The Vapour-phase above the System Sulphuric Acid-Water. *J. Phys. Chem.* **1946**, *50*, 260.

[6] Greenewalt, C. H. Partial pressure of water out of aqueous solutions of sulfuric acid. *Ind. Eng. Chem.* **1925**, *17*, 522-523.

[7] Gmitro, J. I.; Vermeulen, T. Vapor-Liquid Equilibria for Aqueous Sulfuric Acid. *A. I. Ch. E J.* **1964**, *10 No 5*, 740-746.

[8] Wilson, R. W.; Stein, F. P. Correlation of sulfuric acid-water partial pressures. *Fluid Phase Equilib.* **1989**, *53*, 279-288.

[9] Pessoa, F. L. P.; Siqueira Campos, C. E. P.; Uller, A. M. C. Calculation of vapor-liquid equilibria in aqueous sulfuric acid solutions using the UNIQUAC equation in the whole concentration range. *Chemical Engineering Science* **2006**, *61*, 5170-5175.

[10] Bosen, A.; Engels, H. Description of the phase equilibrium of sulfuric acid with the NRTL equation and a solvation model in a wide concentration and temperature range. *Fluid Phase Equilib.* **1988**, *43*, 213-230.

[11] Nist Chemistry WebBook: http://webbook.nist.gov/chemistry/.

[12] Luchinskii, G. P. Physical-chemical Study of the H2O-SO3 System, I. Equilibrium in the vapor and the liquid phase. *Zh. Fiz. Khim.* **1956**, *30*, 1207.

[13] Renon; Prausnitz Local compositions in thermodynamic excess functions for liquid mixtures. *AIChE J.* **1968**, *14*, 135-144.

[14] Hindiyarti, L.; Glarborg, P.; Marshall, P. Reactions of SO3 with the O/H radical pool under combustion conditions. *J. Phys. Chem. A* **2007**, *111*, 3984-3991.

[15] Mueller, P. Dew point temperatures in cylinders of diesel engines working with fuel that contains sulfur (Taupunkttemperaturen im Zylinder von Dieselmaschinen bei schwefelhaltigen Kraftstoffen, Nr 486). *VDI -- Forschungsheft* **1961**, *27*, 1-56.

[16] Ferguson, C. R.; Kirkpatrick, A. T., Eds.; *Internal combustion engines / applied thermosciences;* Wiley: New York, 2001; .

[17] Andreasen, A.; Mayer, S. Modeling of the Oxidation of Fuel Sulfur in Low Speed two-Stroke Diesel Engines. In *26 CIMAC World Congress*; CIMAC: Bergen, 2010; .

[18] Poschl, U.; Canagaratna, M.; Jayne, J. T.; Molina, L. T.; Worsnop, D. R.; Kolb, C. E.; Molina, M. J. Mass Accommodation Coefficient of H2SO4 Vapor on Aqueous Sulfuric Acid Surfaces and Gaseous Diffusion Coefficient of H2SO4 in N2/H2O. *J. Phys. Chem.* **1998**, *102*, 10082.

[19] Reid, R. C.; Sherwood, T. K., Eds.; *The properties of gases and liquids. Their estimation and correlation;* McGraw-Hill Book Company: New York, 1958; .

[20] Land, T. Theory of Acid Deposition and its Application to the Dew-Point Meter. *J. Inst. Fuel* **1977**, *50*, 68-75.